 DOI:10.30420/566414009

Analysis and Design of Asymmetrical Half-bridge (AHB) Flyback Converter

Zhang Guoxing[1] , Bai Pengcheng[2] , Wang Zan[2] , Luo Junyang[1]

[1] Infineon Technologies, Singapore
[2] Infineon Technologies, China

Corresponding author: Zhang Guoxing, Guoxing.Zhang@infineon.com
Speaker: Zhang Guoxing, Guoxing.Zhang@infineon.com

Abstract

This paper presents a detailed analysis of operation principle for AHB Flyback converter. With the ability of ZVS operation for primary-side switches over wide operation range, this topology is a good candidate for high efficiency design as the switching loss can be greatly reduced. A straightforward design procedure is proposed with PFC as front stage for high power chargers and adapters. With Infineon's latest CoolMOS technology and AHB controller, the whole system efficiency can reach 94% at 140W(28V/5A) under 90Vac.

1 Introduction

In the charger and adapter application, high-efficiency and high-power-density are increasingly demanded, which leads to the improvements of switching devices, magnetic components, converter topologies and control technologies. For output power lower than 65W, high-frequency quasi-resonant Flyback converter is widely adopted due to its low cost and good performance. However, with output power increasing, the limitation of conventional Flyback converter is getting more and more obvious: the increasing rating of primary-side device, the bigger size of transformer and the more difficulty of passing EMI.

Since PD application prefers converter with a wide range of output voltage, the usage of LLC resonant converter is limited unless a DC-DC converter is adopted on the secondary side, which increases the total BOM cost and limits the overall efficiency. Thus, the asymmetrical half-bridge (AHB) Flyback converter is getting more attention with its relatively wide gain range, ZVS and ZCS ability, and novel control methods [1-5]. Infineon has released its combo controller XDPS2221 with PFC and AHB for high power PD applications. With this controller, both CoolMOS and GaN devices can be used to achieve high performance designs [1]. The latest generation of CoolMOS and GaN from Infineon contributes to further efficiency enhancement with improved figure-of-merit (FoM).

In this paper, operation principle of AHB Flyback converter is analyzed with different modes. After that, a simple design produce is proposed to build a proper power stage. Finally, a 140W board with CoolMOS in primary side is made to verify the results.

2 AHB Flyback Converter Operation Principle

Fig. 1 shows the circuit diagram of AHB Flyback converter with transformer on the bottom. The primary-side switches Q_1 and Q_2 have a half-bridge configuration, which is connected to the input voltage source V_{IN} and the resonant tank combining resonant capacitor C_r and transformer. The resonant inductance L_r can be provided by the leakage inductance of transformer. Secondary-side diode rectifier or synchronous rectifier (SR) can be either on bottom or top like conventional Flyback converter.

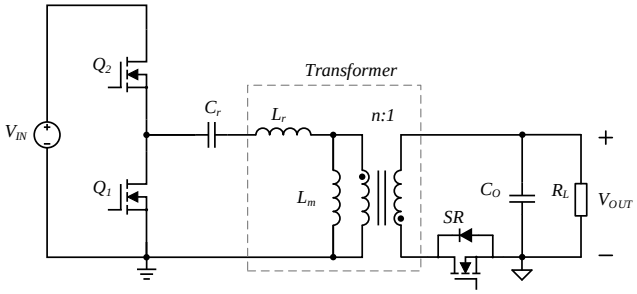

Fig. 1. AHB Flyback Converter Circuit Diagram

2.1 Three Basic Operation Modes

Considering the continuity of magnetizing current, the AHB Flyback converter has three basic operation modes: continuous conduction mode (CCM), critical conduction mode (CRM) and discontinuous conduction mode (DCM). Figure 2 shows these three operation modes. Like conventional Flyback converter, AHB Flyback converter with CCM can deal with higher power,

 DOI:10.30420/566414009

while DCM is a good choice for light load with its reduced switching frequency and CRM is an optimum mode with balanced conduction and switching losses.

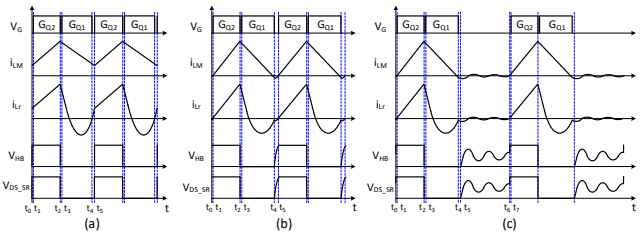

Fig. 2. Three basic operation modes of AHB Flyback converter (a. CCM, b. CRM, c. DCM)

2.1.1 CCM Operation

With CCM operation under steady state, the magnetizing current i_{Lm} of transformer does not reach zero in every switching cycle, which allows higher power transferred from input to output with lower primary-side RMS current. However, CCM operation is not preferred due to reverse recovery of body diode when Si MOSFETs are used for the primary-side switches. The turn-on loss of the main switch increases significantly as well compared to ZVS operation. The high switching loss limits the converter operating with high frequency even with wide-band-gap (WBG) devices. Moreover, CCM operation may introduce more risks of shoot through between the primary-side main switch and secondary-side SR.

2.1.2 CRM Operation

Most of the available controllers are designed to operate the AHB Flyback converter at CRM under heavy load, while DCM under light load as shown in Fig3. Under CRM operation, switching frequency increases with load decreasing, which brings more switching loss and limits the conversion efficiency. Thus, to achieve a better overall efficiency curve, DCM is designed to cover light to middle load range to balance conduction loss and switching loss. For extremely light load, Burst mode is introduced to further boost the efficiency.

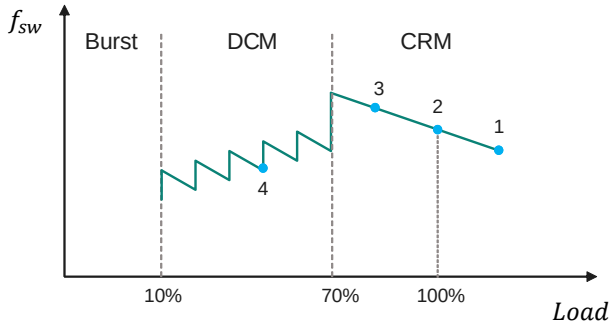

Fig. 3. Controller operation modes vs load

With CRM operation, the magnetizing current reaches zero for every switching cycle. This enables the converter to achieve ZVS operation for primary-side switches based on proper design. Since resonance happens between L_r and C_r during Q_1 turned on, there are possibilities that the resonant current i_{Lr} not reaching (Fig. 4a, point 3 in Fig 3), just meeting (Fig. 4b, point 2 in Fig 3), or already met (Fig. 4c, point 1 in Fig 3) the magnetizing current i_{Lm} when Q_1 turns off as shown in Fig. 4. This is all depending on the matching of resonant period and demagnetizing time of L_m. Considering the relationship between operation modes and load in Fig. 3, it is recommended to position exact CRM (Fig. 4b) around full load point, which could achieve primary-side ZVS and secondary-side ZCS and has relatively small overall RMS current.

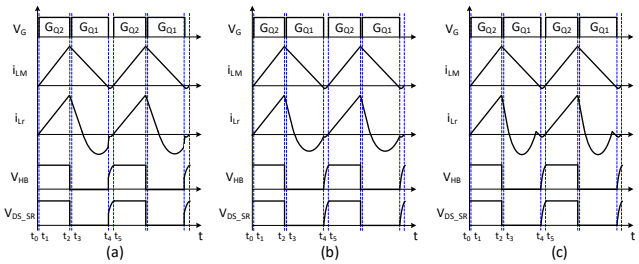

Fig. 4. i_{Lr} and i_{Lm} relationship under CRM at Q_1 off (a. i_{Lr} not reaching i_{Lm}, b. i_{Lr} meeting i_{Lm}, c. i_{Lr} already met i_{Lm})

To better understand the work principle, here takes the exact CRM (Fig. 4b) for a deep analysis. With the i_{Lr} meeting i_{Lm} when Q_1 turns off, the secondary-side rectifier just achieves ZCS turn-off. For this CRM operation, the relationship can be derived as shown in below equations. These equations are based on the waveform continuity in steady state operation.

$$\begin{cases} I_{rOn}\cdot sin(\theta_O/\sqrt{m}+\theta_{O0}) = I_{rNn}\cdot sin(\theta_{N0}) \\ I_{rNn}\cdot sin(\theta_N+\theta_{N0}) = I_{rOn}\cdot sin(\theta_{O0}) \\ -\sqrt{m}\cdot I_{rOn}\cdot cos(\theta_O/\sqrt{m}+\theta_{O0})+1/M = -I_{rNn}\cdot cos(\theta_{N0})+1 \\ -I_{rNn}\cdot cos(\theta_N+\theta_{N0})+1 = -\sqrt{m}\cdot I_{rOn}\cdot cos(\theta_{O0})+1/M \\ I_{rOn}\cdot sin(\theta_{O0}) = I_{rOn}\cdot sin(\theta_O/\sqrt{m}+\theta_{O0})-\theta_N/(m-1) \\ p_{on} = 1/\theta_O+\theta_N\cdot\left(I_{rOn}\cdot sin(\theta_O/\sqrt{m}+\theta_{O0})\cdot\theta_N-\theta_N^2/2\cdot(m-1)+I_{rNn}\cdot(cos(\theta_N+\theta_{N0})-cos(\theta_{N0}))\right) \end{cases}$$

The currents are normalized by $I_{base} = N\cdot V_{OUT}/Z_r$, where $Z_r = \sqrt{L_r/C_r}$, m equals to L_m/L_r, M is the gain $N\cdot V_{OUT}/V_{IN}$, $p_{on} = Z_r/R_L$ and R_L represents the load.

Fig. 5 shows some analysis results from above equations for duty cycle, switching frequency f_{sw}, low-side switch on time t_{on_Q1}, and high-side switch on time t_{on_Q2} with changing input voltage V_{IN} based on a 140W design. The analysis considers a PFC stage in front with V_{IN} varying from 300V to 420V. Duty cycle is almost linearly increasing with V_{IN} decreasing. In fact, the L_m peak current keeps almost constant when switching frequency decreases with V_{IN}. Even the resonant frequency does not change, to keep the converter operate at the exact CRM, the low-side switch on time is slightly decreasing with V_{IN}. On the other hand, the high-side

switch requires more on time to build the magnetizing current with lower V_{IN}.

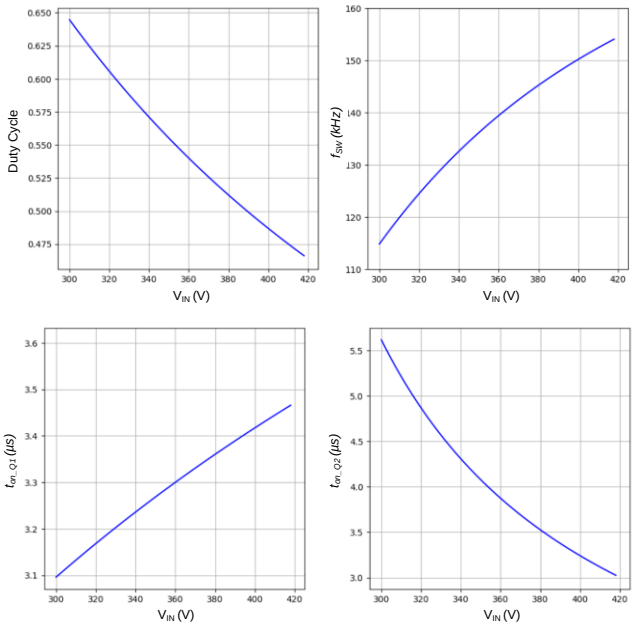

Fig. 5. Duty cycle, switching frequency f_{sw}, t_{on_Q1} and t_{on_Q2} @CRM with i_{Lr} meeting i_{Lm} when Q_1turns off

2.1.3 DCM Operation

With load decreasing, switching frequency increases for the AHB Flyback converter working under CRM. Thus, discontinuous conduction mode (DCM) is introduced as shown in Fig. 3 with the relationship between operation modes and load.

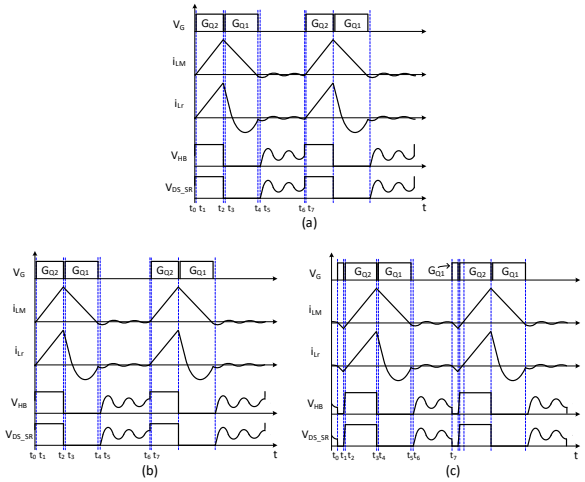

Fig. 6. DCM operation (a. turn on without control, b. turn on at valley, c. Infineon ZV-RVS)

Switching loss can be reduced since frequency fold back is applied under DCM operation. But without further control, the high-side switch may turn on at its high V_{DS}voltage during oscillation as shown in Fig. 6a, which will increase its turn-on loss and bring high volage spike on secondary-side SR. Thus, valley switching can be adopted to improve the turn on the main switch as shown in Fig. 6b. The combo controller XDPS2221 from Infineon has proposed an advanced RV-ZVS control to enable a short ZVS pulse with the low-side switch to ensure a complete ZVS for the high-side switch as shown in Fig. 6c to further reduce the switching loss and eliminate SR spike when high-side switch turns on.

3 New Generation of High-voltage Devices from Infineon

Infineon has launched its new generation of CoolMOS and CoolGaN recently with best-in-class figure of merits and performance in their own technology field.

The new 600V CoolMOS™ 8 SJ MOSFET comes with improved gate charge (Q_g), C_{OSS}, turn-off losses (E_{OSS},), reverse recovery charge (Q_{rr}) and reverse recovery time (t_{rr}) compared to the CFD7 and P7. Fig. 7 shows an example of C_{OSS} and Q_{rr} comparison between CM8, CFD7 and P7. With these improvements, the CoolMOS 8 is a good choice for soft switching topologies as well as PFC converters.

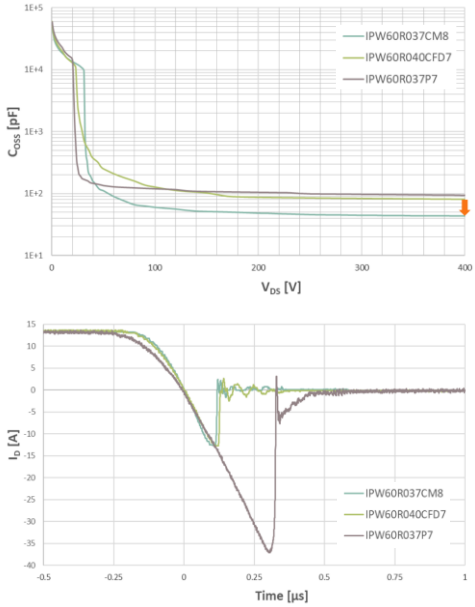

Fig. 7. C_{OSS} and Q_{rr} comparison between CM8, CFD7 and P7

To further enhance the performance of power converters, the wide-band-gap devices, such as GaN, offer even lower switching losses and better thermal performance. Compared to silicon, GaN has a higher electron mobility, facilitating faster and more efficient charging. Its high thermal conductivity enables better heat dissipation, which is crucial for maintaining the compact size of chargers while increasing power delivery capabilities. This aspect is particularly beneficial as it directly addresses the heat dissipation challenges in charger design, aligning with the need for higher power density and efficiency.

 DOI:10.30420/566414009

4 System Design Considerations

From above analysis, the AHB Flyback converter is recommended to design at CRM under maximum rating power. To make easy use of the AHB Flyback converter, a simple design procedure is recommended.

a) The simplified DC gain at CRM can be derived as:

$$V_{OUT} = D * V_{IN}/N$$

where D is the duty cycle of high-side switch and N is transformer turn ratio. With the maximum allowed duty cycle D_{MAX} and range of V_{IN}, transformer turn ratio range can be obtained. Together with secondary-side SR V_{DS_SR} rating requirement ($V_{DS\_SR} = V_{IN}/N$), the selection of turn ratio can be further narrow down.

b) With a minimum required dead time T_D from low-side swich off to high-side switch on, the negative current of transformer magnetic inductance L_m can be calculated as:

$$I_{Lm\_neg} = C_{OSS\_total} * V_{IN\_MAX}/T_D$$

where C_{OSS_total} is the total parasitic capacitance including transformer parasitic capacitance, C_{OSS} of two primary switches and secondary SR. V_{IN_MAX} is the maximum input voltage.

c) The peak current of L_m can be obtained from the following equation based on the relationship of input and output power:

$$I_{OUT} = N\left(I_{Lm\_peak} - I_{Lm\_neg}\right)/2$$

where I_{OUT} is the output current and I_{Lm_peak} is the peak current of Lm. With the defined switching frequency, the selected transformer turn-ratio N, and the calculated Lm peak and negative current, the transformer magnetic inductance Lm can be calculated as:

$$L_m = \frac{N*V_{OUT}*D}{f_{sw}*\left(I_{Lm\_peak}+I_{Lm\_neg}\right)}$$

d) The resonant frequency f_r between L_r and C_r is difficult to have a straight expression, but it can be obtained based on the relationship equations between i_{Lr} and i_{Lm} in one switching cycle. Since L_r is the leakage inductance of the transformer, normally we can use 1.5%-2% of L_m for the first calculation. Thus, the resonant capacitance can be calculated as well:

$$C_r = \frac{1}{4\pi^2 {f_r}^2 L_r}$$

e) With the selected core of transformer, switching frequency, allowed B_{MAX} and turn ratio N, the primary-side and secondary-side windings can be obtained.

With these steps, an initial design of AHB Flyback power stage is finished with transformer and resonant tank parameters. Further optimization can be done during prototype experiment.

5 Experiment Results

Based on the above analysis and design procedure proposed, a 140W reference board is built as shown in Fig. 8. The major components are listed in Table 1.

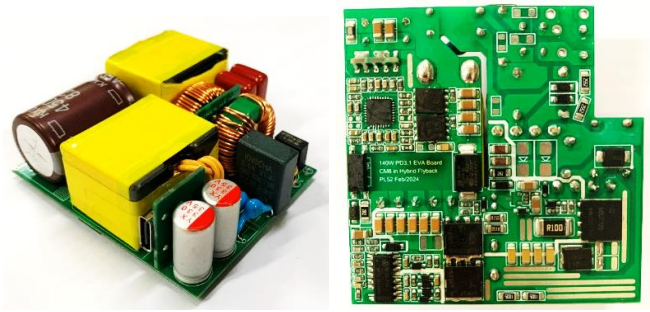

Fig. 8. 140W AHB Flyback Board Pictures

Table 1 140W AHB Flyback Board Major Components

Item	Description
Transformer	21:3, Lm=320μH, Lr=4.2μH
Resonant Cap Cr	330nF/250V*6
Controller	XDPS2221
Primary switch	IPTA60R180CM8*2
SR	ISC0805NLS*2
SR&PD controller	PAG2S

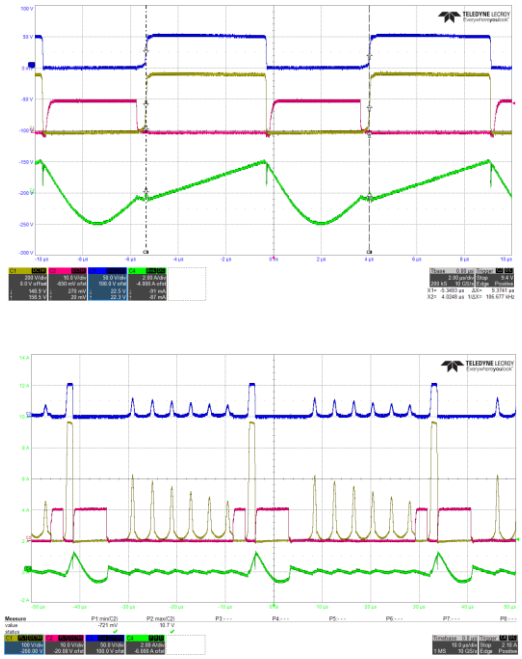

Fig. 9. 140W AHB Flyback Board Pictures

Two typical waveforms are shown in Fig. 9. The AHB Flyback is running at CRM under maximum load (28V5A) as the waveforms on the top. With load decreasing to 5V/1A under 264Vac where PFC stops switching, the AHB converter works at DCM as the waveforms on the bottom. As can be seen, XDPS2221 has a pre-turn on of the low-side switch before the high-side switch on, which creates a negative L_m current for the high-side switch to achieve ZVS. This special designed DCM operation is called RV-ZVS in XDPS2221, which not only reduces turn-on loss of the high-side switch, but also reduces the spike on the secondary SR.

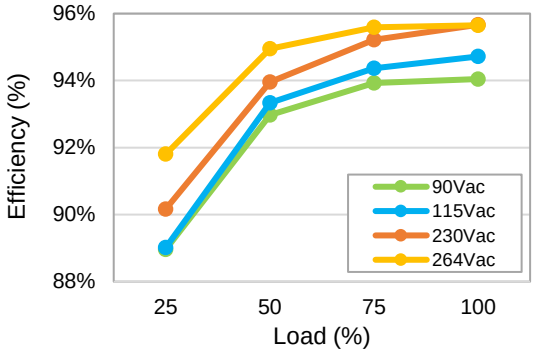

Fig. 10. Measured Efficiency under V_{OUT}=28V

Fig. 10 shows the measured efficiency with V_{OUT} at 28V. The efficiency is above 94% under 90Vac and around 94.7% under 115Vac.

6 Conclusion

In this paper, the AHB Flyback converter has been analysed with operation principle and design procedure. With the ability of ZVS and ZCS operation, and wide DC gain range, it becomes a good candidate for USB PD application. With the new generation of Infineon CoolMOS technology, a 140W reference board is made to achieve high efficiency up to 94% at 90Vac.

7 References

[1] A. Medina-Garcia, F. J. Romero, D. P. Morales, and N. Rodriguez, "Advanced Control Methods for Asymmetrical Half-Bridge Flyback," in IEEE Transactions on Power Electronics, vol. 36, no. 11, pp. 13139-13148, Nov. 2021, doi: 10.1109/TPEL.2021.3077184.

[2] Y. Huang, C. Li, and Y. Chen, "A modified asymmetrical half-bridge flyback converter for step-down ac-dc applications", IEEE Trans. Power Electron., vol. 35, no. 5, pp. 4613-4621, May 2020.

[3] L. Xue and J. Zhang, "Active clamp flyback using GaN power IC for power adapter applications", Proc. IEEE Appl. Power Electron. Conf. Expo., pp. 2441-2448, Mar. 2017.

[4] L. Huber and M. M. Jovanović, "Analysis design and performance evaluation of asymmetrical half-bridge flyback converter for universal-line-voltage-range applications", Proc. IEEE Appl. Power Electron. Conf. Expo., pp. 2481-2487, 2017.

[5] M. Li, Z. Ouyang, and M. A. E. Andersen, "Analysis and optimal design of high-frequency and high-efficiency asymmetrical half-bridge flyback converters", IEEE Trans. Ind. Electron., vol. 67, no. 10, pp. 8312-8321, Oct. 2020.

